ACS APPLIED MATERIALS & INTERFACES

www.acsami.org

Research Article

Time-Separated Pulse Release–Activation of an Enzyme from Alginate–Polyethylenimine Hydrogels Using Electrochemically Generated Local pH Changes

Ilya Sterin, Anna Tverdokhlebova, Evgeny Katz,* and Oleh Smutok*

Cite This: *ACS Appl. Mater. Interfaces* 2024, 16, 28222–28229

Read Online

ACCESS | Metrics & More | Article Recommendations | Supporting Information

ABSTRACT: β-Glucosidase (EC 3.2.1.21) from sweet almond was encapsulated into pH-responsive alginate–polyethylenimine (alginate–PEI) hydrogel. Then, electrochemically controlled cyclic local pH changes resulting from ascorbate oxidation (acidification) and oxygen reduction (basification) were used for the pulsatile release of the enzyme from the composite hydrogel. Activation of the enzyme was controlled by the very same pH changes used for β-glucosidase release, separating these two processes in time. Importantly, the activity of the enzyme, which had not been released yet, was inhibited due to the buffering effect of PEI present in the gel. Thus, only a portion of the released enzyme was activated. Both enzymatic activity and release were monitored by confocal fluorescence microscopy and regular fluorescent spectroscopy. Namely, commercially available very little or nonfluorescent substrate 4-methylumbelliferyl-β-D-glucopyranoside was hydrolyzed by β-glucosidase to produce a highly fluorescent product 4-methylumbelliferone during the activation phase. At the same time, labeling of the enzyme with rhodamine B isothiocyanate was used for release observation. The proposed work represents an interesting smart release–activation system with potential applications in biomedical field.

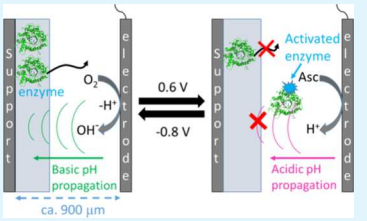

KEYWORDS: *on-demand release, enzymes, hydrogels, electrochemistry, local pH changes*

INTRODUCTION

In the last few decades, smart materials have gotten a lot of attention due to their application in the biomedical field.[1,2] In particular, on-demand (signal-triggered) release was extensively studied for drug delivery purposes.[3,4] Among the triggering factors, one can mention biomolecular signals,[5] magnetic field,[6] mechanical force,[7] temperature,[8] electromagnetic (such as visible light,[9] infrared,[10] and radio[11] waves) radiation, ultrasound,[12] electrical field,[13] and even more sophisticated signals, like breath.[14] One of the most usable triggers for drug delivery is pH[15,16] due to its endogenous nature, which is often associated with a certain disease. For example, it is well-known that tumor tissues are acidified compared to the healthy biological microenvironment.[17]

When modeling smart pH-triggered release systems, one should use pH-sensitive materials which can be based on liposomes,[16] microparticles,[18] nanoparticles,[15] materials modified with pH-sensitive linkers,[19] metal–organic frameworks,[20] and ionic synthetic or natural polymers.[21] One such naturally derived material is alginate, which is a biocompatible and biodegradable ionic polysaccharide made of residues of α-L-guluronic and β-D-mannuronic acids. This material is widely used in the biomedical field.[22] Alginate is able to form a hydrogel when being cross-linked by different metal ions like Ca^{2+}, Ba^{2+}, Sr^{2+}, Fe^{3+}, etc.[23] The weakly acidic nature of the hydrogel allows it to respond to the pH of the surrounding environment. In particular, lowering the pH makes the alginate backbone more protonated, decreasing the overall negative charge of the matrix, while an increase in the pH deprotonates the backbone, increasing the matrix negative charge. This feature was used by many scientists when developing alginate-based smart release systems with a focus on the conventional release profile of encapsulated substances.[24−30] However, only very few works were aimed to achieve a pulsatile release profile of a payload. For example, Raut et al.[31] were using Zn-cross-linked alginate beads, and the pulsatile release was obtained by manual replacement of dissolution media having different pH. In the other work by Kikuchi et al.,[32] alginate beads of different sizes were mixed together, and the difference in time required for dissolution of a certain bead size allowed to obtain a pulse release profile of encapsulated dextran (i.e., no use of alginate pH sensitivity).

Based on our recent work,[33] electrochemically controlled cyclic local pH changes (pH waves) can be used to obtain an on-demand pulsatile release of proteins from alginate hydrogel (and other materials),[34] avoiding the need for manual media replacement and allowing clear real-time observation of the

Received: March 31, 2024
Revised: May 9, 2024
Accepted: May 14, 2024
Published: May 23, 2024

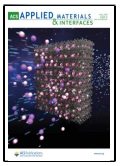

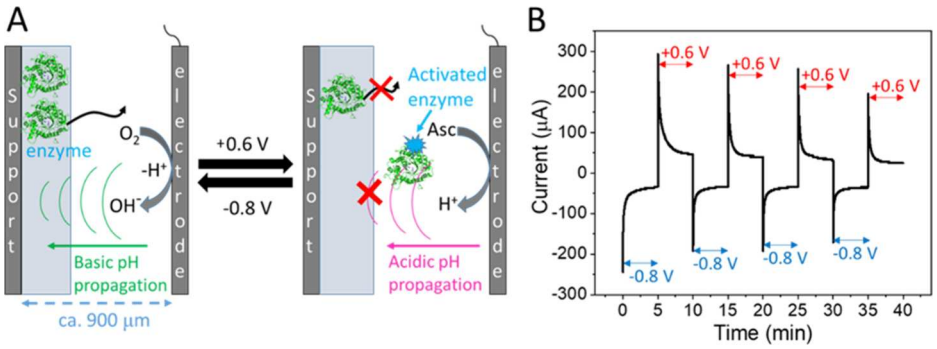

Figure 1. (A) Concept of time-separated pulsatile release and activation of β-glucosidase from the alginate−PEI composite hydrogel using electrochemically generated local pH changes. (B) Chronoamperometry measurements obtained during potential switches: −0.8 V for O_2 reduction and +0.6 V for ascorbate oxidation resulting in local basification and acidification at the electrode surface, respectively (four cycles).

system behavior by means of confocal fluorescence microscopy (CFM). Obtained pulsatile release can be used for extended drug release, which is especially important for the treatment of chronic diseases, allowing reduction of invasive procedures for a patient, better management of drug life cycle, and prolonged symptomatic relief caused by a decrease in fluctuating concentrations of the drug.[35]

Extended release, which is accompanied by an additional control tool aiming at activation/inhibition of the drug that is already released or still encapsulated, would represent an interesting smart release−activation system with potential use in biomedical applications. This is particularly important if one does not want the drug to be active while it is being encapsulated, which can be the case for protease-based therapeutics.[36] In this case, possible self-cleavage will not happen, and the activity of the intact protease will be preserved for its real target.[37,38] Or it can be the case when protease in the form of precursor becomes active upon self-cleavage (both happen at low pH),[39,40] and to avoid it being activated too early, one can maintain a high pH in the carrier. In general, higher pH in the carrier can ensure a lack of unnecessary early activation of a drug, avoiding off-target action-associated toxicity.[41] This is especially relevant for the targets having physiological pH (i.e., pH which is the same as in the healthy environment). This approach will fall in line with already existing pH-dependent therapeutics targeting cancer tumors with the only difference that the tumors' microenvironment pH is lower than the physiological one.[42,43]

As for the object payload, we decided to use β-glucosidase from almonds (EC 3.2.1.21). β-Glucosidase is used as therapeutics in cancer therapy[44−47] and is even considered as a component of an alternative to antibiotics.[48] Deficient β-glucosidase activity is also associated with Gaucher's disease.[49−51] It is known that almond β-glucosidase has a strong pH-dependent activity, which is decreasing at basic pH values.[52] This property can be used for activation and inhibition of the enzyme depending on the pH value. Such characteristics as molecular weight (M_w) of 135 kDa (dimer) and isoelectric point (pI) of 7.3[53] make the enzyme a good object for the pH-triggered on-demand release from alginate hydrogel.[33]

Encapsulation of an enzyme and control of its activity by the very same pH changes used for enzyme release, separating these two processes in time, was the objective of this work.

RESULTS AND DISCUSSION

Principles and Concept. Both the enzymatic activity and release of β-glucosidase can be monitored through fluorescence measurements, simplifying the detection process. Namely, commercially available very little or nonfluorescent substrate 4-methylumbelliferyl-β-D-glucopyranoside (4-MUG) is known to be hydrolyzed by β-glucosidase to produce highly fluorescent product 4-methylumbelliferone (4-MU) (Figure S1).[54,55] At the same time, a simple labeling reaction of the enzyme with rhodamine B isothiocyanate (Figure S2) can be used for release observation. It should be noted that pH dependence of the activity of rhodamine B-labeled enzyme (rh-β-glucosidase or rh-βG) was preserved (Figure S3), and its activity was very close to one of the unlabeled enzyme at pH 5 (Figure S4A). At the same time, rhodamine B-based fluorescence was observed only in the samples of the labeled enzyme, regardless of the presence or absence of the reaction event (Figure S4B). Also, the effect of labeling on a pI value of the enzyme was checked by calculating the dye/protein molar ratio from absorbance measurements of the rh-β-glucosidase sample at 560 nm (rhB tag) and 280 nm (protein) (Figure S5A; calculation details can be found in the Supporting Information). Theoretically, pI change was negligible (ΔpH of 0.1 unit) (Figure S5B), and thus, it should not have been affected the following experiments.

The concept of the project is described in Figure 1A. Support with deposited enzyme-encapsulating hydrogel is positioned in parallel with the working electrode in microscale proximity (Figure S6). Application of −0.8 V (vs Ag/AgCl/KCl) on the working electrode results in oxygen reduction (note the presence of O_2 in the solution in equilibrium with air) and propagation of local basic pH wave toward the hydrogel, stimulating the release of the protein from the hydrogel due to electrostatic repulsion between the protein and hydrogel matrix (both of which are negatively charged). At this step, enzyme activity is inhibited due to the high pH. Then, switching the potential to +0.6.V results in ascorbate oxidation (note that ascorbate was added to the solution in a physiological concentration) and propagation of a local acidic wave, inhibiting the release due to the increasing impact of electrostatic attraction between the enzyme and the hydrogel matrix. At the same time, acidic pH should activate the enzyme. Cyclic potential switches (−0.8 V ↔ +0.6 V) were done to obtain pulsatile release−activation behavior. Typical chronoamperometry is shown in Figure 1B. Importantly, we did not want the acidic wave to penetrate inside the gel in

https://doi.org/10.1021/acsami.4c05273
ACS Appl. Mater. Interfaces 2024, 16, 28222−28229

order to keep the encapsulated enzyme inactive. The acidic wave should activate only the portion of the enzyme that was released in the solution during the previous phase.

PEI Effect on pH Behavior in the Composite Hydrogel. Therefore, for enzyme encapsulation, we decided to use a composite hydrogel[56−58] composed of alginate (2% w/v) and high M_w branched polyethylenimine (PEI) (0.5% v/v). The rheology test confirmed the gel state of the material (gelation was done in $CaCl_2$ solution) since storage modulus G′ was higher than the loss modulus G' in the linear viscoelastic region (Figure S7A). FTIR of the formed hydrogel showed the presence of carbonyl groups of alginate (signal at around 1650 cm^{-1}) as well as a broad signal between 3000 and 4000 indicating NH and OH groups (Figure S7B). PEI is a cationic polymer consisting of multiple amino groups. It is used in drug delivery[59,60] and possesses antimicrobial properties.[61,62] PEI is also known to have buffer capacity in the basic pH region.[63,64] Thus, the PEI presence in the hydrogel did not allow the acidic wave to propagate inside the gel, clearly separating the pH environment inside and outside of the gel. This can be observed using CFM through fluorescence of pH-sensitive fluorescent dye, 3,4′-dihydroxy-3′,5′-bis-(dimethylaminomethyl)flavone (FAM345) (fluorescence increases in basic solutions)[65] with the gel being brighter (higher pH) than the outside solution (lower pH) (Figure 2A, Movie S1). Using calibration based on FAM345 brightness at different pH values (Figure S8), we could estimate pH changes inside and outside the gel (Figure 2B). It should be noted that the effect of PEI on both FAM345 fluorescence and β-glucosidase activity was checked to exclude any possibility of results misinterpretations. In particular, FAM345 fluorescence was not very different in solutions of PEI and the 2-amino-2-methylpropanol (AMP) buffer with the same pH, with the fluorescence signal being higher in the buffer (Figure S9). Therefore, the same calibration was used when estimating the pH inside and outside the gel. At the same time, the maximum pH-dependent activity of the enzyme was slightly shifted in the basic pH direction in the presence of PEI, which made us choose pH 9.5 as a starting buffer pH for the experiment (Figure S10).

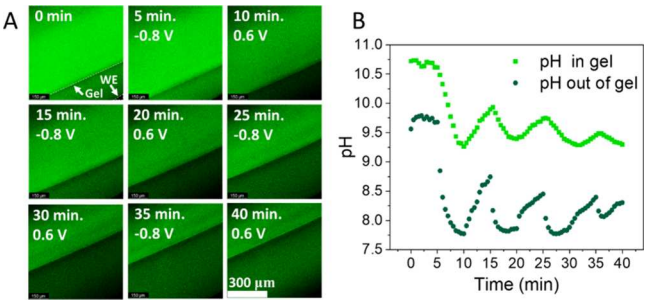

Figure 2. (A) Confocal fluorescence microscope images of the alginate−PEI composite hydrogel and neighboring solution layer obtained from the experiment on electrochemical generation of cyclic local pH changes (−0.8 V (basic pH) ↔ +0.6 V (acidic pH), 5 min each cycle) propagating from working electrode (WE) using pH-sensitive FAM345 dye; (B) pH changes in the gel (light green) and the outside solution (dark green) were estimated using brightness-based calibration of FAM345 at different pH.

Pulse Release of β-Glucosidase from the Composite Hydrogel. Upon consumption of bulk solution H^+ ions by PEI amino groups, a positive charge in the gel is created. This allows for electrostatic attraction between the hydrogel matrix and still encapsulated enzyme (note that pH in the gel does not go below pI of β-glucosidase, so enzyme net charge is still negative), resulting in its release inhibition (Figure 3).

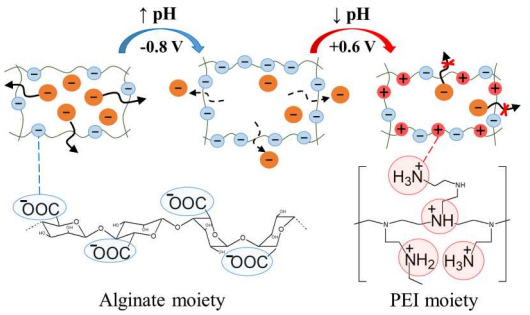

Figure 3. Schematics showing electrostatic interactions in the system upon basification and acidification. Release of β-glucosidase (orange circles) is promoted upon the increase in the hydrogel (alginate−PEI composite) matrix negative charge due to deprotonation of alginate carboxylic groups. Release is inhibited upon the increase in the hydrogel matrix positive charge due to protonation of PEI amino groups. Inserted are the chemical structures of alginate and PEI to demonstrate their charges.

CFM images showing the pulsatile release of rh-β-glucosidase upon electrochemically induced local pH changes are shown in Figure 4A (also see Movie S2). It should be noted that rhodamine B fluorescence is pH-independent in the pH range of our interest[66] and should not have been affected by the release observations. Figure 4B shows a corresponding change in rhB tag brightness in the solution part, which is neighboring the hydrogel (pink cloud below the gel).

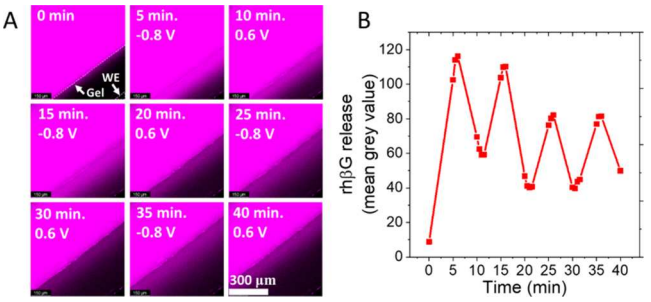

Figure 4. (A) Confocal fluorescence microscope images of composite alginate−PEI hydrogel with encapsulated rh-β-glucosidase showing its pulsatile release from the gel upon electrochemical generation of cyclic local pH changes (−0.8 V (basic pH) ↔ +0.6 V (acidic pH), 5 min each cycle) propagating from the working electrode (WE); (B) rh-β-glucosidase pulsatile release from the gel based on the brightness of pink cloud in the solution layer neighboring the gel.

Pulse Activation of β-Glucosidase Released from the Composite Hydrogel. The next experiments were aimed at monitoring β-glucosidase enzymatic activity with CFM using 4-MUG as a fluorescent substrate. The brightness-based results are shown in Figure 5 and Movie S3. As it was expected, the 4-MU product was produced in the solution during the acidification stages (brightness increased), but enzyme activity was inhibited during the basification stages of the solution (brightness stayed the same). Note that an increase in fluorescence brightness at the very first pH change stage (basification) may originate from residual 4-MUG fluores-

https://doi.org/10.1021/acsami.4c05273
ACS Appl. Mater. Interfaces 2024, 16, 28222−28229

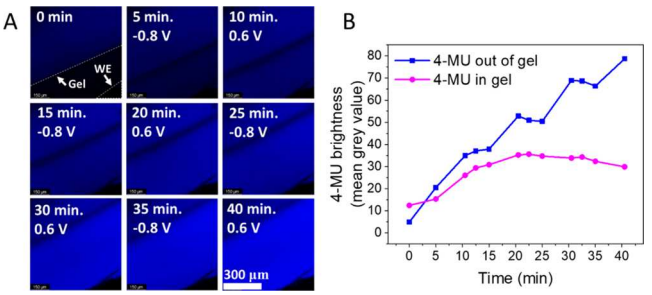

Figure 5. (A) Confocal fluorescence microscope images of composite alginate−PEI hydrogel with encapsulated β-glucosidase showing pulsatile production of 4-MU in solution upon activation of previously released (−0.8 V (basic pH), 5 min each cycle) β-glucosidase by electrochemically generated acidic local pH changes (+0.6 V, 5 min each cycle) propagating from the working electrode (WE); (B) 4-MU fluorescence in the solution layer neighboring the gel (blue) and in the gel (pink) that was converted to brightness to show pulsatile activation of β-glucosidase released to the solution.

cence, which is increasing at basic pH[67,68] or from minor enzymatic activity of β-glucosidase. To avoid misinterpretation of the results originating from pH-dependence fluorescence of 4-MU, the image representing the end of an acidification cycle (activation phase) was taken shortly after switching the potential to −0.8 V in order to switch to the basic pH (note that there is no change in the brightness at the end of the acidification cycle and at the end of the following basification cycle, meaning that the short time of basic pH switching is sufficient to obtain adequate results; otherwise, we would see a huge fluorescence response at the end of the basification cycle). It should be noted that brightness change in the gel mostly stayed at a plateau throughout the whole experiment. Initial gel brightness can be explained by its higher pH since 4-MUG that diffused inside the gel has pH-dependent residual fluorescence and also by some minor enzymatic activity of β-glucosidase reacting with 4-MUG diffused inside the gel. However, with time brightness of the solution neighboring the gel becomes significantly larger compared to the inside-the-gel one, indicating that the enzyme in the gel is not being activated, while enzymatic reaction kinetics is faster than the diffusion of produced 4-MU from the outside solution into the gel.

Quantification of Pulse Release/Activation of β-Glucosidase. While brightness-based results on the release and activation are a good qualitative indicator of the system, the quantitative assessment would be even more representative. For that, experiments described above were done with fraction collection at the end of each acidification/basification cycle, and fluorescence spectroscopy measurements were performed and transformed to the quantitative information using calibration curves based on rhodamine B tag or 4-MU fluorescence at different amounts of the enzyme (Figure S11). After the collection, the pH in each fraction was adjusted to pH 10.5 to stop the reaction and obtain the best fluorescence response of the produced 4-MU. The results summarizing release and activation with the corresponding pH changes are shown in Figure 6A.

It is clearly seen that at the pH increase, the release of the enzyme is stimulated while its activity is inhibited, whereas at the pH decrease, the opposite effect is observed. The quantitative evaluation also allowed us to estimate the participation of not yet released β-glucosidase in the enzymatic activation process. This was done using the calibration based on 4-MU fluorescence obtained after 5 min of enzymatic reaction of different enzyme amounts at pH 7.9 (the amount of substrate in the reaction accounted for the activation of the 10 μg of the enzyme during each activation phase since 10 μg of the enzyme was encapsulated in the gel). As shown in Figure 6B, the experimental curve (blue) is much closer to the theoretical curve which would be obtained in the case when the acidic wave would not penetrate inside the gel (pink curve, in-gel enzyme is not activated) when compared to the theoretical curve that would be obtained with the acidic wave penetration inside the gel (brown curve, in-gel enzyme is activated).

CONCLUSIONS

In this work, time-separated pulsatile release and activation of β-glucosidase was achieved by means of cyclic electrochemically generated local pH changes. It was possible to avoid activation of β-glucosidase that was still encapsulated in the gel via gel buffering by the PEI presence in the composite material. Proposed work can be particularly relevant if one does not want the drug to be active while being encapsulated to avoid off-target associated toxicity. Higher pH in the carrier, which was ensured in this work by the presence of PEI, can be especially relevant for the targets that have physiological pH (i.e., pH which is the same as in the healthy environment). This approach will fall in line with already existing pH-dependent therapeutics targeting cancer tumors with the only

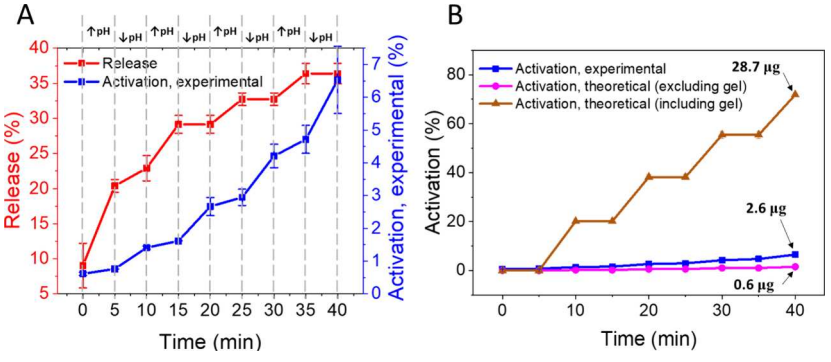

Figure 6. (A) Time-separated pulsatile release (red) and activation (blue) of rh-β-glucosidase resulting from cyclic electrochemically generated local pH changes. (B) Experimentally obtained activation curve as well as theoretical activation curves that would be obtained if the acidic wave would (brown) or would not (pink) penetrate inside the gel.

https://doi.org/10.1021/acsami.4c05273
ACS Appl. Mater. Interfaces 2024, 16, 28222−28229

difference being that the tumors' microenvironment pH is lower than the physiological one. In general, the study described above can be coupled with molecular biology research aiming at tuning the pH-dependent activity of therapeutic enzymes/proteins.

EXPERIMENTAL SECTION

General Instrumentation. Fluorescent images were obtained with a Leica TCS SP5 II Tandem Scanning Confocal and Multiphoton microscope (Figure S12). Animated movies were compiled by using GIMP software. The brightness of FAM345, rhodamine B-labeled β-glucosidase, and 4-MU in the images was evaluated with ImageJ software, calculating the mean gray value of the equal area in each image. A Shimadzu UV-2450 UV−vis spectrophotometer was used to measure the absorbance spectrum of rh-β-glucosidase. Fluorescence measurements were performed in a 96-well microplate by using a SpectraMax MiniMax 300 Imaging Cytometer (Molecular Devices) and SoftMax Pro 6 software. A Mettler Toledo S20 SevenEasy pH meter was used to measure the pH of the solutions. Cyclic voltammetry and constant-potential chronoamperometry experiments were performed by using an electrochemical workstation (ECO Chemie Autolab PASTAT 10) and GPES 4.9 (General Purpose Electrochemical System) software. FTIR spectrum was collected with a Thermo Scientific Nicolet iS10 infrared FTIR spectrometer. Rheology test (amplitude sweep) was performed with an Anton Paar modular compact rheometer MCR 302.

Chemicals and Reagents Used. Alginic acid sodium salt from brown algae (Sigma-Aldrich), β-glucosidase from almonds (EC 3.2.1.21, Sigma-Aldrich), rhodamine B isothiocyanate (Sigma-Aldrich), poly(ethylenimine) 50% (w/v) solution in H_2O (M_w = 60 kDa, M_w = 750 kDa, Sigma-Aldrich), 4-methylumbelliferyl β-D-glucopyranoside (Sigma-Aldrich), 2-amino-2-methylpropanol (AMP buffer, Sigma-Aldrich), calcium chloride anhydrous (Thermo Fisher Scientific), sodium ascorbate (Sigma-Aldrich), hydrochloric acid (Thermo Fisher Scientific), sodium hydroxide (Thermo Fisher Scientific), sodium carbonate (Thermo Fisher Scientific), sodium bicarbonate (Thermo Fisher Scientific), Sephadex G-50 (Cytiva), glycine (VWR), and sodium chloride (Sigma-Aldrich). pH-sensitive fluorescent dye 3,4′-dihydroxy-3′,5′-bis(dimethylaminomethyl)-flavone (FAM345) was synthesized according to the procedures reported in the literature.[65,69] Ultrapure water (18.2 MΩ cm) from a NANOpure Diamond (Barnstead) source was used in all experiments.

Labeling of β-Glucosidase with Rhodamine B Isothiocyanate. β-Glucosidase and rhodamine B isothiocyanate were separately dissolved in carbonate−bicarbonate buffer, pH 9.2. The enzyme solution was kept in an ice bath, and the solution of the dye was added in a dropwise manner. The molar ratio of dye/enzyme in the reaction mixture was 24.5/1. The reaction mixture was allowed to stir for 6 h in the ice bath. Then, the mixture was separated by gel filtration using an equilibrated column filled with Sephadex G-50 particles. The labeled enzyme (rh-β-glucosidase) band was collected and further concentrated using Spin-X UF Concentrator, Corning, with 100 kDa cutoff. The obtained sample was measured using UV−vis spectroscopy to determine the enzyme concentration and dye/enzyme ratio.

Preparation of the Alginate−PEI Composite Hydrogel. PEI solution was added, and sodium alginate was dissolved in the solution of 0.1 M Na_2SO_4 in H_2O. The mixture was allowed to be stirred overnight. The final mixture composition was 0.5% PEI (v/v), and 2% sodium alginate (w/v) (for example, for 5 mL mixture, one should dissolve 100 mg of sodium alginate in 4.95 mL of 0.1 M Na_2SO_4 and add 0.050 mL of commercially available 50% (w/v) solution of PEI). The composite hydrogel was prepared by applying the needed volume (16 μL) of the mixture onto the horizontally fixed graphite sheet electrode (used simply as a support, width of 4 mm, area covered by the hydrogel 42 mm^2) and cross-linking in 20 mM $CaCl_2$ in AMP buffer, pH 9.5, for 2 min. The obtained deposited hydrogel was rinsed with distilled water and used in further experiments.

Composite Hydrogel Characterization. To confirm the gel-like nature of the gel, shear-strain-amplitude sweep was performed. Measurements were done by using plate geometry. The experiment was carried out at a frequency of 10 Hz and deformations ranging from 0.01 to 100. The hydrogel was cross-linked for 2 min and was carefully placed onto the lower plate surface, and the upper plate was lowered to a 1 mm gap distance.

FTIR spectroscopy measurements were performed to identify functional groups of the hydrogel in the range from 4000 to 1300 cm^{-1}. Spectrum was collected by putting dried hydrogel film onto a NaCl disk, which is typically used for FTIR measurements.

Fluorescence Spectroscopy Measurements during Release−Activation Experiments. Ten μg amount of rh-β-glucosidase was encapsulated in the gel. The solution composition was 1.8 mM 4-MUG, 2.5 mM sodium ascorbate, and oxygen in equilibrium with air in 1 mM AMP buffer, pH 9.5. To measure fluorescence, the solution was thoroughly mixed after each basification/acidification phase, and 100 μL samples were collected into a 96-well plate. Immediately after collection, 50 μL of 0.5 M glycine, 0.125 M Na_2CO_3, and 0.1 M NaCl, pH 10.5, was added to each sample (to stop the enzymatic reaction and avoid pH dependence of 4-MU fluorescence). Then, fluorescence was assessed on an Imaging Cytometer (microplate reader). The settings on the microplate reader were as follows:

1. Rhodamine B label (release): excitation λ_{ex} 540 nm, emission recorded between 565 and 605 nm. The emission maximum was observed at 575 nm. The measurement step was 10 nm.
2. 4-MU settings (activation): λ_{ex} 365 nm, emission recorded between 425 and 465 nm. Emission maximum was observed at 455 nm. The measurement step was 10 nm.

To estimate the release percentage, calibration based on rhodamine B label fluorescence at different rh-β-glucosidase concentrations was used.

To estimate the activation percentage, the calibration based on 4-MU fluorescence obtained after 5 min of enzymatic reaction at pH 7.9 of different enzyme amounts was used (the amount of 4-MUG in the reaction accounted for the activation of the 10 μg of the enzyme during each activation phase; the pH of samples was adjusted to 10.5 for the measurement).

Electrochemical Experiments. All potentials were measured against Ag/AgCl/KCl, 3 M reference electrode.

Cyclic voltammetry experiments were performed in a regular electrochemical cell. The graphite sheet electrode was used as a working electrode (geometrical area exposed to the solution ca. 0.68 cm^2), and a graphite rod (diameter 3 mm) was used as a counter electrode (geometrical area exposed to the solution ca. 1.1 cm^2). The electrolyte solution was 0.5 mM Na_2SO_4 in 1 mM AMP buffer, pH 9.5. Sodium ascorbate (when present) concentration was 2.5 mM, and oxygen (when not removed under an argon atmosphere) was dissolved in equilibrium with air. The potential scan rate for all cyclic voltammetry experiments was 50 mV/s.

The typical experiment on pH visualization, rh-β-glucosidase release, or activation was done in a Petri dish with a plasticine barrier used as an improvised electrochemical cell (see Figure S6). CFM imaging was performed during the electrochemical experiments. A single experiment was done using four sequential reduction−oxidation cycles. The potential switch program (a multistep chronoamperometry setup) used to induce local pH changes is shown in Table 1.

Solution composition during experiments on CFM:

1. pH visualization experiment: 2.5 mM sodium ascorbate, oxygen in equilibrium with air, 10 μM FAM345 in 1 mM AMP buffer, pH 9.5;
2. rh-β-glucosidase release experiment: 2.5 mM sodium ascorbate, oxygen in equilibrium with air in 1 mM AMP buffer, pH 9.5;
3. Enzyme activation experiment: 1.8 mM 4-MUG, 2.5 mM sodium ascorbate, oxygen in equilibrium with air in 1 mM AMP buffer, pH 9.5.

https://doi.org/10.1021/acsami.4c05273
ACS Appl. Mater. Interfaces 2024, 16, 28222−28229

Table 1. Potential Program for the Release−Activation Experiments

cycles	steps	potential applied, V[a]	time interval, min
1	1st basification	−0.8	5
	1st acidification	+0.6	5
2	2nd basification	−0.8	5
	2nd acidification	+0.6	5
3	3rd basification	−0.8	5
	3rd acidification	+0.6	5
4	4th basification	−0.8	5
	4th acidification	+0.6	5

[a]Chronoamperometry setup was used in the experiments.

Measurement of pH-Dependent Activity of rh-β-Glucosidase. The same amount of rh-β-glucosidase was dissolved in the wells containing AMP buffer (final buffer concentration of 5 mM) with pH ranging from 3 to 11 (step of 1 pH unit) in a 96-well microplate. Then, 4-MUG was added to each well at the same concentration to start the enzymatic reaction. The reaction was allowed to proceed for 15 min, after which a stop solution of 0.5 M glycine, 0.125 M Na_2CO_3, and 0.1 M NaCl, pH 10.5, was added to each well. Then, fluorescence spectroscopy measurements on a microplate reader as well as CFM observations were performed. The settings were as follows:

Microplate reader: λ_{ex} 365 nm, emission recorded between 425 and 465 nm;
Confocal microscope: λ_{ex} 405 nm, emission recorded between 410 and 500 nm.

Processing of Images. Animated movies were prepared using GIMP software. The brightness of FAM345, rhodamine B-labeled β-glucosidase, and 4-MU in the CFM images was evaluated with ImageJ software, calculating the mean gray value of the equal area in each image. For the evaluation of pH values inside/outside of the gel, the calibration based on the brightness of FAM345 images obtained at different pH (7−11, step of 1 pH unit) in AMP buffer was used.

All experiments were performed at ambient room temperature, ca. 20−22 °C.

■ ASSOCIATED CONTENT

Data Availability Statement

The data that support the findings of this study are available from the corresponding author upon reasonable request.

Supporting Information

The Supporting Information is available free of charge at https://pubs.acs.org/doi/10.1021/acsami.4c05273.

Enzymatic hydrolysis; chemical reaction between the primary amino group of β-glucosidase lysine residue side chain and isothiocyanate group attached to the rhodamine B fluorescent dye; pH dependence of rh-β-glucosidase enzymatic activity; activity of rhodamine B-labeled and unlabeled β-glucosidase; rhodamine B fluorescence of labeled and unlabeled β-glucosidase; absorbance spectrum of rh-β-glucosidase; estimation of the pI values of rh-β-glucosidase; experimental setup of the developed release−activation system; amplitude sweep test; FTIR measurements; FAM345 confocal fluorescence microscope images; pH-dependent fluorescence of FAM345; calibration based on rhodamine B tag fluorescence; calibration based on 4-MU fluorescence and experimental setup combining a scanning confocal fluorescence microscope and a potentiostat (PDF)

Movie 1: Animated image showing the difference in pH environment in the hydrogel and the outside solution created upon electrochemical generation of cyclic local pH changes (MOV)

Movie 2: Animated image showing the pulsatile release of rh-β-glucosidase from the hydrogel upon electrochemical generation of cyclic local pH changes (MOV)

Movie 3: Animated image showing the pulsatile production of 4-MU in solution upon activation of β-glucosidase portion which was previously released from the hydrogel (MOV)

■ AUTHOR INFORMATION

Corresponding Authors

Oleh Smutok − *Department of Chemistry and Biomolecular Science, Clarkson University, Potsdam, New York 13699, United States;* orcid.org/0000-0002-9967-3445; Email: osmutok@clarkson.edu

Evgeny Katz − *Department of Chemistry and Biomolecular Science, Clarkson University, Potsdam, New York 13699, United States;* orcid.org/0000-0002-1618-4620; Email: ekatz@clarkson.edu

Authors

Ilya Sterin − *Department of Chemistry and Biomolecular Science, Clarkson University, Potsdam, New York 13699, United States;* orcid.org/0000-0002-4960-496X

Anna Tverdokhlebova − *Department of Chemistry and Biomolecular Science, Clarkson University, Potsdam, New York 13699, United States;* orcid.org/0000-0002-4531-2193

Complete contact information is available at: https://pubs.acs.org/10.1021/acsami.4c05273

Author Contributions

The manuscript was written through the contributions of all authors. All authors have given approval to the final version of the manuscript.

Notes

The authors declare no competing financial interest.

■ ACKNOWLEDGMENTS

The authors thank Dr. Richard Chandradat for the help in carrying out the rheology test and Dr. Galina Melman for the advice on FTIR measurements. This work was supported by US National Science Foundation (NSF) grant CBET-2235349 including IMPRESS-U supplement to E.K.

■ ABBREVIATIONS

PEI, polyethylenimine; M_w, molecular weight; 4-MU, 4-methylumbelliferone; 4-MUG, 4-methylumbelliferyl-p-D-glucopyranoside; CFM, confocal fluorescence microscopy; FAM345, 3,4′-dihydroxy-3′,5′-bis(dimethylaminomethyl)-flavone; AMP, 2-amino-2-methylpropanol; FTIR, Fourier-transform infrared spectroscopy

■ REFERENCES

(1) Najjari, A.; Aghdam, R. M.; Ebrahimi, S. A. S.; Suresh, K. S.; Krishnan, S.; Shanthi, C.; Ramalingam, M. Smart piezoelectric biomaterials for tissue engineering and regenerative medicine: a review. *Biomed. Technol.* **2022**, *67* (2), 71−88.

(2) Aflori, M. Smart nanomaterials for biomedical applications − a review. *Nanomaterials* **2021**, *11* (2), 396.
(3) Xiong, Y.; Qi, L.; Niu, Y.; Lin, Y.; Xue, Q.; Zhao, Y. Autonomous drug release systems with disease symptom-associated triggers. *Adv. Intell. Syst.* **2020**, *2*, No. 1900124.
(4) Sun, T.; Dasgupta, A.; Zhao, Z.; Nurunnabi, M.; Mitragotri, S. Physical triggering strategies for drug delivery. *Adv. Drug Delivery Rev.* **2020**, *158*, 36−62.
(5) Cong, X.; Chen, J.; Xu, R. Recent progress in bio-responsive drug delivery systems for tumor therapy. *Front. Bioeng. Biotechnol.* **2022**, *10*, No. 916952.
(6) Nguyen, D. T.; Nguyen, N. M.; Vu, D. M.; Tran, M. D.; Ta, V. T.; Thuyet, D. Q. On-demand release of drug from magnetic nanoparticle-loaded alginate beads. *J. Anal. Methods Chem.* **2021**, *2021*, No. 5576283.
(7) Hu, X.; Zeng, T.; Husic, C. C.; Robb, M. J. Mechanically triggered release of functionally diverse molecular payloads from masked 2-furylcarbinol derivatives. *ACS Cent. Sci.* **2021**, *7* (7), 1216−1224.
(8) Akash, S. Z.; Lucky, F. Y.; Hossain, M.; Bepari, A. K.; Rahman, G. M. S.; Reza, H. M.; Sharker, S. M. Remote temperature-responsive parafilm dermal patch for on-demand topical drug delivery. *Micromachines (Basel)* **2021**, *12* (8), 975.
(9) Zhang, W.; Ji, T.; Li, Y.; Zheng, Y.; Mehta, M.; Zhao, C.; Liu, A.; Kohane, D. S. Light-triggered release of conventional local anesthetics from a macromolecular prodrug for on-demand local anesthesia. *Nat. Commun.* **2020**, *11*, 2323.
(10) Cao, Y.; Dumani, D. S.; Hallam, K. A.; Emelianov, S. Y.; Ran, H. Real-time monitoring of NIR-triggered drug release from phase-changeable nanodroplets by photoacoustic/ultrasound imaging. *Photoacoustics* **2023**, *30*, No. 100474.
(11) Bariana, M.; Aw, M. S.; Moore, E.; Voelcker, N. H.; Losic, D. Radiofrequency-triggered release for on-demand delivery of therapeutics from titania nanotube drug-eluting implants. *Nanomedicine* **2014**, *9* (8), 1263−1275.
(12) Delaney, L. J.; Isguven, S.; Eisenbrey, J. R.; Hickok, N. J.; Forsberg, F. Making waves: how ultrasound-targeted drug delivery is changing pharmaceutical approaches. *Mater. Adv.* **2022**, *3*, 3023−3040.
(13) Wang, M. L.; Chamberlayne, C. F.; Xu, H.; Mofidfar, M.; Baltsavias, S.; Annes, J. P.; Zare, R. N.; Arbabian, A. On-demand electrochemically controlled compound release from an ultrasonically powered implant. *RSC Adv.* **2022**, *12*, 23337−23345.
(14) Wiegandt, F. C.; Froriep, U. P.; Müller, F.; Doll, T.; Dietzel, A.; Pohlmann, G. Breath-triggered drug release system for preterm neonates. *Pharmaceutics* **2021**, *13*, 657.
(15) Wibowo, F. R.; Saputra, O. A.; Lestari, W. W.; Koketsu, M.; Mukti, R. R.; Martien, R. pH-Triggered drug release controlled by poly(styrene sulfonate) growth hollow mesoporous silica nanoparticles. *ACS Omega* **2020**, *5* (8), 4261−4269.
(16) Langton, M. J.; Scriven, L. M.; Williams, N. H.; Hunter, C. A. Triggered release from lipid bilayer vesicles by an artificial transmembrane signal transduction system. *J. Am. Chem. Soc.* **2017**, *139* (44), 15768−15773.
(17) Bogdanov, A.; Bogdanov, A.; Chubenko, V.; Volkov, N.; Moiseenko, F.; Moiseyenko, V. Tumor acidity: From hallmark of cancer to target of treatment. *Front. Oncol.* **2022**, *12*, No. 979154.
(18) Kumar, A.; Montemagno, C.; Choi, H. J. Smart microparticles with a pH-responsive macropore for targeted oral drug delivery. *Sci. Rep.* **2017**, *7*, 3059.
(19) Timmers, M.; Weterings, J.; Geijn, M.; Bell, R.; Lenting, P. E.; Rijcken, C. F.; Vermonden, T.; Hennink, W. E.; Liskamp, R. M. J. A new class of tunable acid-sensitive linkers for native drug release based on the trityl protecting group. *Bioconjugate Chem.* **2022**, *33* (9), 1707−1715.
(20) Maranescu, B.; Visa, A. Applications of metal-organic frameworks as drug delivery systems. *Int. J. Mol. Sci.* **2022**, *23* (8), 4458.
(21) Singh, J.; Nayak, P. pH-Responsive polymers for drug delivery: Trends and opportunities. *J. Polym. Sci.* **2023**, *61* (22), 2828.
(22) Tomić, S. L.; Babić Radić, M. M.; Vuković, J. S.; Filipović, V. V.; Nikodinovic-Runic, J.; Vukomanović, M. Alginate-based hydrogels and scaffolds for biomedical applications. *Mar. Drugs* **2023**, *21* (3), 177.
(23) Malektaj, H.; Drozdov, A. D.; deClaville Christiansen, J. Mechanical properties of alginate hydrogels cross-linked with multivalent cations. *Polymers* **2023**, *15* (14), 3012.
(24) Oshi, M. A.; Lee, J.; Kim, J.; Hasan, N.; Im, E.; Jung, Y.; Yoo, J.-W. pH-Responsive alginate-based microparticles for colon-targeted delivery of pure cyclosporine a crystals to treat ulcerative colitis. *Pharmaceutics* **2021**, *13* (9), 1412.
(25) Zou, Z. A sodium alginate-based sustained-release IPN hydrogel and its applications. *RSC Adv.* **2020**, *10*, 39722−39730.
(26) Schoeller, J.; Itel, F.; Wuertz-Kozak, K.; Gaiser, S.; Luisier, N.; Hegemann, D.; Ferguson, S. J.; Fortunato, G.; Rossi, R. M. pH-Responsive chitosan/alginate polyelectrolyte complexes on electrospun plga nanofibers for controlled drug release. *Nanomaterials* **2021**, *11* (7), 1850.
(27) Mun, A.; Simaan Yameen, H.; Edelbaum, G.; Seliktar, D. Alginate hydrogel beads embedded with drug-bearing polycaprolactone microspheres for sustained release of paclobutrazol. *Sci, Rep.* **2021**, *11*, 10877.
(28) Dodero, A.; Alberti, S.; Gaggero, G.; Ferretti, M.; Botter, R.; Vicini, S.; Castellano, M. An up-to-date review on alginate nanoparticles and nanofibers for biomedical and pharmaceutical applications. *Adv. Mater. Interfaces* **2021**, *8*, No. 2100809.
(29) Feyisa, Z.; Gupta, N. K.; Edossa, G. D.; Sundaramurthy, A.; Kapoor, A.; Inki, L. G. Fabrication of pH-sensitive double cross-linked sodium alginate/chitosan hydrogels for controlled release of amoxicillin. *Polym. Eng. Sci.* **2023**, *63* (8), 2546−2564.
(30) Abourehab, M. A. S. Alginate as a promising biopolymer in drug delivery and wound healing: a review of the State-of-the-Art. *Int. J. Mol. Sci.* **2022**, *23* (16), 9035.
(31) Raut, N. S.; Deshmukh, P. R.; Umekar, M. J.; Kotagale, N. R. Zinc cross-linked hydroxamated alginates for pulsed drug release. *Int. J. Pharm. Investig.* **2013**, *3* (4), 194−202.
(32) Kikuchi, A.; Kawabuchi, M.; Sugihara, M.; Sakurai, Y.; Okano, T. Pulsed dextran release from calcium-alginate gel beads. *J. Controlled Release* **1997**, *47* (1), 21−29.
(33) Tverdokhlebova, A.; Sterin, I.; Darie, C. C.; Katz, E.; Smutok, O. Stimulation−inhibition of protein release from alginate hydrogels using electrochemically generated local pH changes. *ACS Appl. Mater. Interfaces* **2022**, *14* (51), 57408−57418.
(34) Sterin, I.; Hadynski, J.; Tverdokhlebova, A.; Masi, M.; Katz, E.; Wriedt, M.; Smutok, O. Electrochemical and biocatalytic signal-controlled payload release from a metal−organic framework. *Adv. Mater.* **2024**, *36*, No. 2308640.
(35) Kalaydina, R. V.; Bajwa, K.; Qorri, B.; Decarlo, A.; Szewczuk, M. R. Recent advances in "smart" delivery systems for extended drug release in cancer therapy. *Int. J. Nanomed.* **2018**, *13*, 4727−4745.
(36) Craik, C. S.; Page, M. J.; Madison, E. L. Proteases as therapeutics. *Biochem. J.* **2011**, *435* (1), 1−16.
(37) Kapust, R. B.; Tözsér, J.; Fox, J. D.; Anderson, D. E.; Cherry, S.; Copeland, T. D.; Waugh, D. S. Tobacco etch virus protease: mechanism of autolysis and rational design of stable mutants with wild-type catalytic proficiency. *Protein Eng., Des. Sel.* **2001**, *14* (12), 993−1000.
(38) Harris, C. L. Generation of anti-complement "prodrugs": cleavable reagents for specific delivery of complement regulators to disease sites. *J. Biol. Chem.* **2003**, *278* (38), 36068−36076.
(39) Blair, W. S.; Semler, B. L. Self-cleaving proteases. *Curr. Opin. Cell. Biol.* **1991**, 3 (6), 1039−1045.
(40) Berry, A. J. Pancreatic enzyme replacement therapy during pancreatic insufficiency. *Nutr. Clin. Pract.* **2014**, *29*, 312−321.
(41) Marsh, M. C.; Owen, S. C. Therapeutic fusion proteins. *AAPS J.* **2024**, *26*, 3.

(42) Klaus, T.; Deshmukh, S. pH-Responsive antibodies for therapeutic applications. *J. Biomed. Sci.* **2011**, *28* (1), 11.
(43) Malik, E.; Dennison, S. R.; Harris, F.; Phoenix, D. A. pH Dependent antimicrobial peptides and proteins, their mechanisms of action and potential as therapeutic agents. *Pharmaceuticals* **2016**, *9* (4), 67.
(44) Martin, H.; Ramırez Lazaro, L.; Gunnlaugsson, T.; Scanlan, E. M. Glycosidase activated prodrugs for targeted cancer therapy. *Chem. Soc. Rev.* **2022**, *51*, 9694−9716.
(45) Li, Yl; Li, Qx; Liu, Rj; Shen, Xq Chinese medicine amygdalin and β-glucosidase combined with antibody enzymatic prodrug system as a feasible antitumor therapy. *Chin. J. Integr. Med.* **2018**, *24*, 237−240.
(46) Zhou, J.; Hou, J.; Rao, J.; Zhou, C.; Liu, Y.; Gao, W. Magnetically directed enzyme/prodrug prostate cancer therapy based on β-glucosidase/amygdalin. *Int. J. Nanomedicine* **2020**, *15*, 4639−4657.
(47) Girivel, H. Beta glucosidase in enzyme and prodrug cancer therapy. *J. Biotechnol. Biomater.* **2022**, *12*, 283.
(48) Volozhantsev, N. V.; Borzilov, A. I.; Shpirt, A. M.; Krasilnikova, V. M.; Verevkin, V. V.; Denisenko, E. A.; Kombarova, T. I.; Shashkov, A. S.; Knirel, Y. A.; Dyatlov, I. A. Comparison of the therapeutic potential of bacteriophage KpV74 and phage-derived depolymerase (β-glucosidase) against *Klebsiella pneumoniae* capsular type K2. *Virus Res.* **2022**, *322*, No. 198951.
(49) Sawkar, A. R.; Cheng, W. C.; Beutler, E.; Wong, C. H.; Balch, W. E.; Kelly, J. W. Chemical chaperones increase the cellular activity of N370S β-glucosidase: A therapeutic strategy for Gaucher disease. *Proc. Natl. Acad. Sci. U.S.A.* **2002**, *99* (24), 15428−15433.
(50) Beutler, E.; Kuhl, W. Detection of the defect of gaucher's disease and its carrier state in peripheral-blood leucocytes. *Lancet* **1970**, *295* (7647), 612−613.
(51) Hultberg, B.; Sjöblad, S.; Öckerman, P. A. 4-Methylumbelliferyl-β-glucosidase in cultured human fibroblasts from controls and patients with gaucher's disease. *Clin. Chim. Acta* **1973**, *49* (1), 93−97.
(52) Papalazaridou, A.; Charitidou, L.; Sivropoulou, A. β-Glucosidase enzymatic activity of crystal polypeptide of the *Bacillus thuringiensis* strain 1.1. *J. Endotoxin Res.* **2003**, *9* (4), 215−224.
(53) Grover, A. K.; MacMurchie, D. D.; Cushley, R. J. Studies on almond emulsin βd-glucosidase I. Isolation and characterization of a bifunctional isozyme. *Biochim. Biophys. Acta* **1977**, *482* (1), 98−108.
(54) Mead, J. A.; Smith, J. N.; Williams, R. T. Studies in detoxication. 67. The biosynthesis of the glucuronides of umbelliferone and 4-methylumbelliferone and their use in fluorimetric determination of beta-glucuronidase. *Biochem. J.* **1955**, *61* (4), 569−574.
(55) Graf, F. M. R.; Buchhaupt, M. Comparative investigations on different β-glucosidase surrogate substrates. *Fermentation* **2022**, *8* (2), 83.
(56) Dangi, Y. R.; Lin, X.; Choi, J. W.; Lim, C. R.; Song, M. H.; Han, M.; Bediako, J. K.; Cho, C. W.; Yun, Y. S. Polyethyleneimine functionalized alginate composite fiber for fast recovery of gold from acidic aqueous solutions. *Environ. Technol. Innovation* **2022**, *28*, No. 102605.
(57) Xu, R.; Su, C.; Cui, L.; Zhang, K.; Li, J. Preparing sodium alginate/polyethyleneimine spheres for potential application of killing tumor cells by reducing the concentration of copper ions in the lesions of colon cancer. *Materials* **2019**, *12* (9), 1570.
(58) Dangi, Y. R.; Bediako, J. K.; Lin, X.; Choi, J. W.; Lim, C. R.; Song, M. H.; Han, M.; Yun, Y. S. Polyethyleneimine impregnated alginate capsule as a high capacity sorbent for the recovery of monovalent and trivalent gold. *Sci. Rep.* **2021**, *11*, 17836.
(59) Limiti, E.; Mozetic, P.; Giannitelli, S. M.; Pinelli, F.; Han, X.; Rio, D.; Abbruzzese, F.; Basoli, F.; Rosanò, L.; Scialla, S.; Trombetta, M.; Gigli, G.; Zhang, Z. J.; Mauri, E.; Rainer, A. Hyaluronic acid−polyethyleneimine nanogels for controlled drug delivery in cancer treatment. *ACS Appl. Nano Mater.* **2022**, *5* (4), 5544−5557.
(60) Zakeri, A.; Kouhbanani, M. A. J.; Beheshtkhoo, N.; Beigi, V.; Mousavi, S. M.; Hashemi, S. A. R.; Zade, A. K.; Amani, A. M.; Savardashtaki, A.; Mirzaei, E.; Jahandideh, S.; Movahedpour, A. Polyethylenimine-based nanocarriers in co-delivery of drug and gene: a developing horizon. *Nano Rev. Exp.* **2018**, *9* (1), No. 1488497.
(61) Akif, F. A. Polyethylenimine increases antibacterial efficiency of chlorophyllin. *Antibiotics (Basel)* **2022**, *11* (10), 1371.
(62) Gibney, K. A.; Sovadinova, I.; Lopez, A. I.; Urban, M.; Ridgway, Z.; Caputo, G. A.; Kuroda, K. Poly(ethylene imine)s as antimicrobial agents with selective activity. *Macromol. Biosci.* **2012**, *12* (9), 1279−1289.
(63) Harpe, A.; Petersen, H.; Li, Y.; Kissel, T. Characterization of commercially available and synthesized polyethylenimines for gene delivery. *J. Control. Release* **2000**, *69* (2), 309−322.
(64) Choi, E.; Kim, S. Surface pH buffering to promote degradation of mesoporous silica nanoparticles under a physiological condition. *J. Colloid Interface Sci.* **2019**, *533*, 463−470.
(65) Valuk, V. F.; Duportail, G.; Pivovarenko, V. G. A wide-range fluorescent pH-indicator based on 3-hydroxyflavone structure. *J. Photochem. Photobiol., A* **2005**, *175* (2−3), 226−231.
(66) Smart, P. L.; Laidlaw, I. M. S. An evaluation of some fluorescent dyes for water tracing. *Water Resour. Res.* **1977**, *13* (1), 15−33.
(67) Goodwin, R. H.; Kavanagh, F. The fluorescence of coumarin derivatives as a function of pH. II. *Arch. Biochem. Biophys.* **1952**, *36* (2), 442−455.
(68) Bobey, D. G.; Ederer, G. M. Rapid detection of yeast enzymes by using 4-methylumbelliferyl substrates. *J. Clin. Microbiol.* **1981**, *13* (2), 393−394.
(69) Bollella, P.; Melman, A.; Katz, E. Operando local ph mapping of electrochemical and bioelectrochemical reactions occurring at an electrode surface: Effect of the buffer concentration. *ChemElectroChem.* **2021**, *8*, 3923.

https://doi.org/10.1021/acsami.4c05273
ACS Appl. Mater. Interfaces 2024, 16, 28222−28229